Position-independent normal-mode splitting in cavities filled with zero-index metamaterials

Hai-tao Jiang,[1,*] Xiao-hu Xu,[1] Zi-li Wang,[1] Yun-hui Li,[1] Yasha Yi,[2,3] and Hong Chen[1]

[1]*Key Laboratory of Advanced Micro-structure Materials, MOE, Department of Physics, Tongji University, Shanghai 200092, China*

[2]*Integrated Nanophotonics Laboratory, NYU and CUNY Graduate Center, New York, New York 10016, USA*

[3]*Massachusetts Institute of Technology, Cambridge, Massachusetts 02139, USA*

**jiang-haitao@tongji.edu.cn*

Abstract: We study the normal-mode splitting when an oscillator is placed in a two-dimensional photonic crystal microcavity embedded with an impedance-matched or an impedance-mismatched zero-index medium (ZIM). Because of the (nearly) uniform localized fields in the ZIM, the normal-mode splitting remains (almost) invariant no matter where the oscillator is. When a split ring resonator is coupled to a transmission-line-based effective ZIM at various locations, nearly position-independent mode splitting is observed.

OCIS codes: (270.5580) Quantum electrodynamics; (160.3918) Metamaterials; (160.5298) Photonic crystals.

References and links

1. P. Berman, ed., *Cavity Quantum Electrodynamics* (Academic, 1994).
2. J. M. Raimond, M. Brune, and S. Haroche, "Manipulating quantum entanglement with atoms and photons in a cavity," Rev. Mod. Phys. **73**(3), 565–582 (2001).
3. A. Blais, R. S. Huang, A. Wallraff, S. M. Girvin, and R. J. Schoelkopf, "Cavity quantum electrodynamics for superconducting electrical circuits: An architecture for quantum computation," Phys. Rev. A **69**(6), 062320 (2004).
4. A. Wallraff, D. I. Schuster, A. Blais, L. Frunzio, R. S. Huang, J. Majer, S. Kumar, S. M. Girvin, and R. J. Schoelkopf, "Strong coupling of a single photon to a superconducting qubit using circuit quantum electrodynamics," Nature **431**(7005), 162–167 (2004).
5. J. P. Reithmaier, G. Sek, A. Löffler, C. Hofmann, S. Kuhn, S. Reitzenstein, L. V. Keldysh, V. D. Kulakovskii, T. L. Reinecke, and A. Forchel, "Strong coupling in a single quantum dot-semiconductor microcavity system," Nature **432**(7014), 197–200 (2004).
6. T. Yoshie, A. Scherer, J. Hendrickson, G. Khitrova, H. M. Gibbs, G. Rupper, C. Ell, O. B. Shchekin, and D. G. Deppe, "Vacuum Rabi splitting with a single quantum dot in a photonic crystal nanocavity," Nature **432**(7014), 200–203 (2004).
7. K. Hennessy, A. Badolato, M. Winger, D. Gerace, M. Atatüre, S. Gulde, S. Fält, E. L. Hu, and A. Imamoğlu, "Quantum nature of a strongly coupled single quantum dot-cavity system," Nature **445**(7130), 896–899 (2007).
8. K. Aoki, D. Guimard, M. Nishioka, M. Nomura, S. Iwamoto, and Y. Arakawa, "Coupling of quantum-dot light emission with a three-dimensional photonic crystal nanocavity," Nat. Photonics **2**(11), 688–692 (2008).
9. L. Sapienza, H. Thyrrestrup, S. Stobbe, P. D. Garcia, S. Smolka, and P. Lodahl, "Cavity quantum electrodynamics with Anderson-localized modes," Science **327**(5971), 1352–1355 (2010).
10. G. Khitrova, H. M. Gibbs, F. Jahnke, M. Kira, and S. W. Koch, "Nonlinear optics of normal-mode-coupling semiconductor microcavities," Rev. Mod. Phys. **71**(5), 1591–1639 (1999).
11. R. W. Ziolkowski, "Propagation in and scattering from a matched metamaterial having a zero index of refraction," Phys. Rev. E Stat. Nonlin. Soft Matter Phys. **70**(4), 046608 (2004).
12. A. Lakhtakia, "Scattering by a nihility sphere," Microw. Opt. Technol. Lett. **48**(5), 895–896 (2006).
13. A. Alù, M. G. Silveirinha, A. Salandrino, and N. Engheta, "Epsilon-near-zero metamaterials and electromagnetic sources: Tailoring the radiation phase pattern," Phys. Rev. B **75**(15), 155410 (2007).

#159017 - $15.00 USD Received 1 Dec 2011; revised 25 Jan 2012; accepted 1 Mar 2012; published 5 Mar 2012

14. B. Edwards, A. Alù, M. E. Young, M. Silveirinha, and N. Engheta, "Experimental verification of epsilon-near-zero metamaterial coupling and energy squeezing using a microwave waveguide," Phys. Rev. Lett. **100**(3), 033903 (2008).
15. K. Halterman and S. M. Feng, "Resonant transmission of electromagnetic fields through subwavelength zero- ε ," Phys. Rev. A **78**(2), 021805 (2008).
16. J. M. Hao, W. Yan, and M. Qiu, "Super-reflection and cloaking based on zero index metamaterial," Appl. Phys. Lett. **96**(10), 101109 (2010).
17. V. C. Nguyen, L. Chen, and K. Halterman, "Total transmission and total reflection by zero index metamaterials with defects," Phys. Rev. Lett. **105**(23), 233908 (2010).
18. H. T. Jiang, Z. L. Wang, Y. Sun, Y. H. Li, Y. W. Zhang, H. Q. Li, and H. Chen, "Enhancement of (nearly) homogeneous fields in a (effective) zero-index cavity," J. Appl. Phys. **109**(7), 073113 (2011).
19. A. J. Hoffman, L. Alekseyev, S. S. Howard, K. J. Franz, D. Wasserman, V. A. Podolskiy, E. E. Narimanov, D. L. Sivco, and C. Gmachl, "Negative refraction in semiconductor metamaterials," Nat. Mater. **6**(12), 946–950 (2007).
20. M. Tokushima, H. Yamada, and Y. Arakawa, "1.5-μm-wavelength light guiding in waveguides in square-lattice-of-rod photonic crystal slab," Appl. Phys. Lett. **84**(21), 4298 (2004).
21. Computer Simulation Technology (CST), User's Manual 5, in CST-Microwave Studio, 2003.
22. P. Holmström, L. Thylén, and A. Bratkovsky, "Dielectric function of quantum dots in the strong confinement regime," J. Appl. Phys. **107**(6), 064307 (2010).
23. I. C. Khoo, D. H. Werner, X. Liang, A. Diaz, and B. Weiner, "Nanosphere dispersed liquid crystals for tunable negative-zero-positive index of refraction in the optical and terahertz regimes," Opt. Lett. **31**(17), 2592–2594 (2006).
24. D. H. Werner, D. H. Kwon, I. C. Khoo, A. V. Kildishev, and V. M. Shalaev, "Liquid crystal clad near-infrared metamaterials with tunable negative-zero-positive refractive indices," Opt. Express **15**(6), 3342–3347 (2007).
25. X. Q. Huang, Y. Lai, Z. H. Hang, H. H. Zheng, and C. T. Chan, "Dirac cones induced by accidental degeneracy in photonic crystals and zero-refractive-index materials," Nat. Mater. **10**(8), 582–586 (2011).
26. K. Aydin, I. Bulu, K. Guven, M. Kafesaki, C. M. Soukoulis, and E. Ozbay, "Investigation of magnetic resonances for different split-ring resonator parameters and designs," New J. Phys. **7**, 168 (2005).
27. L. W. Zhang, Y. W. Zhang, Y. P. Yang, H. Q. Li, H. Chen, and S. Y. Zhu, "Experimental observation of Rabi splitting in effective near-zero-index media in the microwave regime," Phys. Rev. E Stat. Nonlin. Soft Matter Phys. **78**(3), 035601 (2008).
28. D. Y. Lu, H. Liu, T. Li, S. M. Wang, F. M. Wang, S. N. Zhu, and X. Zhang, "Creation of a magnetic plasmon polariton through strong coupling between an artificial magnetic atom and the defect state in a defective multilayer microcavity," Phys. Rev. B **77**(21), 214302 (2008).

1. Introduction

How an atom behaves in a cavity is an interesting problem. The behavior of the atom depends on the coupling strength g between the atomic transition and the photon. If the electric field per photon inside the cavity is large enough, the g can exceed the decay rates of the cavity and the atom. In this case, a doublet in the frequency domain, whose spectral width corresponds to vacuum Rabi splitting, would appear [1]. The observation of vacuum Rabi splitting is considered to be a sign of strong coupling regime of cavity quantum electrodynamics. In the strong coupling regime, the optical properties of the truly quantum system can be modified by the addition of a single photon or single atom, which could be applied in the quantum entanglement, computations and information [2–4]. With the progress of semiconductor technology, a quantum emitter in a cavity changes from an atom to an atomic-like two-level system such as a quantum dot (QD) and the strong coupling of light-matter is realized in the solid-state experiments. For example, vacuum Rabi splitting is observed when a single QD is embedded in a semiconductor micropillar cavity [5] or photonic crystal (PhC) nanocavities [6–9] with high quality factor and small volume. In the classical limit, when a quantum emitter in a cavity changes to a classical oscillator, the overall system response will yield two split modes, which corresponds to the normal-mode splitting in a mechanic language, see reference [10] and references therein. For both vacuum Rabi splitting and normal-mode splitting, the optical cavity modes involved are all in the form of standing waves and the localized fields are inhomogeneous. To ensure strong coupling of a quantum emitter and photons, one needs to place the quantum emitter right at the cavity field maximum, which is very challenging during

#159017 - $15.00 USD Received 1 Dec 2011; revised 25 Jan 2012; accepted 1 Mar 2012; published 5 Mar 2012

fabrication. To overcome the positional uncertainty, in this paper we propose a cavity filled with zero-index metamaterial (ZIM) in which the fields are uniform to realize position-independent mode splitting. Implementing this proposal would alleviate experimental problems caused by the random spatial distributions of self-assembled QDs in a cavity.

A ZIM in which the permittivity $\varepsilon = 0$ and/or the permeability $\mu = 0$ can modify the transport properties of electromagnetic (EM) waves significantly [11–18]. For example, a ZIM can tailor the radiation patterns [13] and squeeze EM waves [14,15]. In an impedance-matched ZIM ($\varepsilon = \mu = 0$), both phases and amplitudes of the EM fields are homogeneous [11]. However, in a ε -near-zero (ENZ) medium ($\varepsilon = 0$, $\mu = 1$, an impedance-mismatched ZIM), although the phases of EM waves are uniform, in most cases the amplitudes of electric fields will spatially vary. In practice, a highly doped semiconductor can be utilized as an ENZ medium at infrared frequencies [19] and QDs might be embedded in this ENZ medium. So how to realize uniform electric fields in an ENZ medium is an important practical problem. In section 2 of this paper, we put an oscillator that can describe the resonant susceptibility of a QD in the strong confinement regime into a ZIM embedded in a two-dimensional (2D) PhC cavity. The enhanced uniform electric fields in an impedance-matched ZIM ensure spatially independent normal-mode splitting. We further discover that, confined by a suitable photonic barrier, the enhanced electric fields can still be almost uniform in an ENZ medium, as required by Maxwell equations and boundary conditions. The nearly uniform electric fields lead to a nearly position-independent normal-mode splitting. Moreover, we discuss the possibility of extending the 2D structure to a three-dimensional (3D) case. Then, in section 3 we fabricate a split ring resonator coupled to a transmission-line-based effective ZIM and observe the nearly position- independent normal-mode splitting. Finally, we conclude in section 4.

2. Normal-mode splitting in 2D ZIM-filled cavities

The schematic of a 2D square-lattice PhC microcavity in x-y plane is shown in Fig. 1. The parameters of the 2D PhC are chosen to be the same with those used in actual experiments [20]. Silicon nanorods with refractive index of 3.48 are embedded in the background polymer with refractive index of 1.45. The rod axis is along z direction and the radius of the rod is 114.6 nm. The lattice constant is 430 nm. The cavity is formed by removing five rods at the center of the 2D PhC. The blue dotted circle with radius of 220 nm indicates a ZIM region surrounded by a 2D photonic barrier. Transverse-electric modes in which the electric fields are along the rod axis are considered. We use a computer simulation technology (CST) microwave studio software based on a finite integration method to do simulations [21]. We select the transient solver in the software to perform full wave simulations. At first, the cavity does not contain a ZIM. We find a resonance mode at the frequency of 188.8 terahertz (THz) and calculate the corresponding mode pattern. As seen from the 2D electric field pattern ($|E_z|$) in Fig. 2(a), a dipolar mode appears. The amplitude of the incident electric field is supposed to be 1 (in arbitrary units). In Fig. 2(b), we also show the magnetic field pattern at 188.8 THz. It is seen that, outside and near the edge of the circle indicated by the dotted line, the values of magnetic fields are very small. Next, we put an oscillator with diameter of 16 nm into the cavity. In the region occupied by the oscillator, the permittivity of the background medium is assumed to be 2.1. The resonant susceptibility of the oscillator is described by

$$\chi_{res} = -\frac{G}{(\omega - \omega_0) + i\gamma_1}, \tag{1}$$

where G , ω_0 and γ_1 denote the strength, the resonance frequency and the loss of the oscillator, respectively, and ω is angular frequency. In the strong confinement regime, Eq. (1) can be used to describe the resonant susceptibility of a QD [22]. In the following calculations,

#159017 - $15.00 USD Received 1 Dec 2011; revised 25 Jan 2012; accepted 1 Mar 2012; published 5 Mar 2012

we assume that $G = 20 \times 2\pi$ THz, $\gamma_1 = 6 \times 2\pi$ THz, and ω_0 coincides with the frequency of cavity mode. We calculate the average intensity of electric fields (in arbitrary units) within the red dotted elliptical zone indicated in Fig. 1 to show the modes of the structure.

The 2D PhC cavity can physically be seen as oscillator 2. When oscillator 1 described by Eq. (1) is put inside the cavity, the system can be treated as two coupled oscillators. Oscillator 1 is driven by the cavity field and oscillator 2 is driven by the external field. The overall response of two coupled oscillators will yield two split modes. Since the radius of oscillator 1 is much smaller than that of the cavity, oscillator 1 can be considered as a point at position (x_0, y_0). The charges $q_1(t)$ and $q_2(t)$ in oscillators 1 and 2 meet the coupled differential equations:

$$\ddot{q}_1(t) + \gamma_1 \dot{q}_1(t) + \omega_0^2 q_1(t) + \kappa(q_1 - q_2) = E(x_0, y_0) e^{i\omega t}, \tag{2}$$

$$\ddot{q}_2(t) + \gamma_2 \dot{q}_2(t) + (\omega_0 + \delta)^2 q_2(t) - \kappa(q_1 - q_2) = E_0 e^{i\omega t}, \tag{3}$$

where κ is the coupling coefficient between the two oscillators, $E(x_0, y_0)$ and E_0 denote the local electric field at the place of oscillator 1 and the external electric field, respectively, γ_2 denotes the loss of oscillator 2 (the decay rate of the cavity), and δ denotes the detuning of the resonance frequency of oscillator 2 from oscillator 1. From Eqs. (2) and (3), one can see that the modes of the two coupled oscillators are affected by the local field $E(x_0, y_0)$. The cavity mode pattern, i.e., the distribution of $E(x_0, y_0)$ inside the cavity, determines the spatial dependence of the split modes. In Fig. 2 the cavity mode is a conventional standing wave that spatially varies. As a result, the split modes will depend on the position of oscillator 1. To avoid the position-dependent normal-mode splitting, one needs to make the local field $E(x_0, y_0)$ homogeneous inside the cavity. To obtain this goal, we put a ZIM indicated by the circular zone in Fig. 1 into the cavity. The permittivity and permeability of a ZIM are described by [16, 17]

$$\varepsilon = \mu = 1 - \frac{\omega_p^2}{\omega(\omega + i\Gamma)}, \tag{4}$$

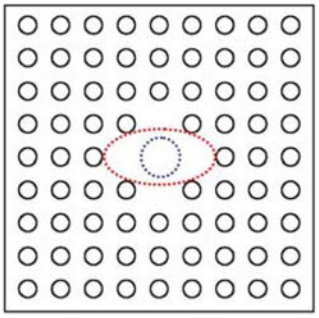

Fig. 1. Schematic of a 2D square-lattice PhC cavity in x-y plane. The radius and refractive index of the silicon rods in background polymer are 114.6 nm and 3.48, respectively. The refractive index of polymer is 1.45 and the lattice constant is 430 nm. The blue dotted circle with radius of 220 nm denotes a ZIM region and the red dotted ellipse denotes a zone for calculating intensities.

#159017 - $15.00 USD Received 1 Dec 2011; revised 25 Jan 2012; accepted 1 Mar 2012; published 5 Mar 2012

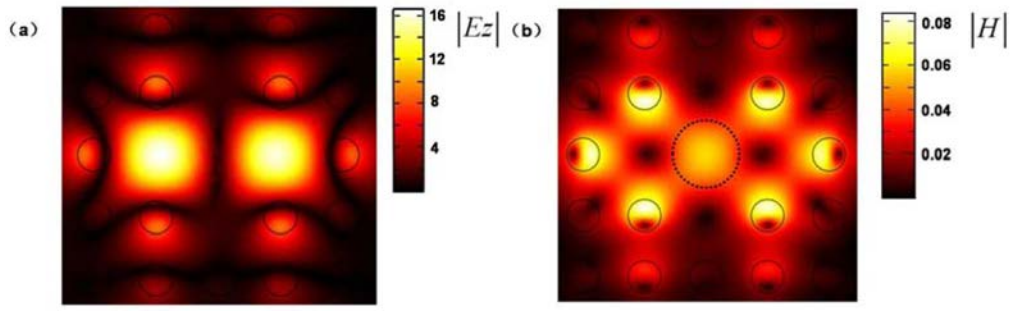

Fig. 2. 2D electric field pattern (a) and magnetic field pattern (b) at a cavity mode of 188.8 THz. The radius of the circle indicated by the dotted line is 220 nm.

where $\omega_p = 175.4 \times 2\pi$ THz and $\Gamma = 2\pi$ GHz. In practice, metamaterials based on liquid crystal can realize low loss ZIMs [23,24]. Moreover, a 2D PhC with accidental degeneracy can mimic a nearly lossless ZIM [25]. From the Maxwell equations, the uniform electric (magnetic) fields inside a ZIM are guaranteed by the $\mu = 0$ ($\varepsilon = 0$) condition. When the refractive index of the defect medium changes from 1.45 to 0, the frequency of the cavity mode shifts to 175.4 THz. In Figs. 3(a) and 3(b), we show the 2D electric field pattern and magnetic field pattern at 175.4 THz, respectively. From Fig. 3(a) one can see the electric fields within the ZIM are largest and uniform. Since the ZIM is surrounded by a region in which the values of magnetic fields are very small, the uniform magnetic fields inside the ZIM are required to be near zero by the boundary condition, as is shown in Fig. 3(b). Then, we put oscillator 1 at arbitrary places of the ZIM and calculate the corresponding average intensity of electric fields. Numerical results show that the mode splitting is independent of the position of oscillator 1.

For a more realistic cavity, we change the impedance-matched ZIM to an ENZ medium in which $\varepsilon = 1 - \dfrac{\omega_p^2}{\omega(\omega + i\Gamma)}$ and $\mu = 1$, respectively [13–15]. In practice, the plasma frequency of free carriers in a doped semiconductor can be tuned by varying the doping density [19]. At the plasma frequency the doped semiconductor can be used as an ENZ medium and self-assembled or colloidal QDs might be embedded in this ENZ medium. After we embed an ENZ medium with $\omega_p = 175.4 \times 2\pi$ THz and $\Gamma = 2\pi$ GHz in the cavity, a resonance mode of 175.4 THz appears. Similar to Fig. 3(b), the value of magnetic fields inside the ENZ medium is forced to be a near-zero constant by the $\varepsilon = 0$ and the boundary conditions. From the Maxwell

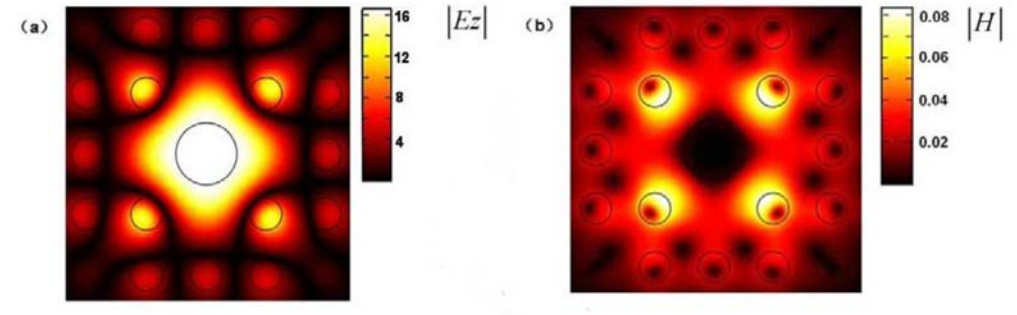

Fig. 3. 2D electric field pattern (a) and magnetic field pattern (b) at a cavity mode of 175.4 THz. The circular zone denotes a ZIM within which the fields are largest and uniform.

#159017 - $15.00 USD Received 1 Dec 2011; revised 25 Jan 2012; accepted 1 Mar 2012; published 5 Mar 2012

equation $\mathbf{H} = \frac{\nabla \times \mathbf{E}}{i\omega\mu_0\mu}$, although $\mu \neq 0$, the electric field $\mathbf{E}$ inside the ENZ medium is required to be almost no changed in space to keep the magnetic field $\mathbf{H}$ as a near-zero constant. In Fig. 4 we show 2D and 3D electric field patterns at 175.4 THz. It is seen that inside the ENZ medium the enhanced electric fields are almost uniform. Outside the edge of the ENZ medium, the electric fields fluctuate a little bit. Next, we put an oscillator described by Eq. (1) at three different places in the ENZ medium as indicated by the white, the black and the gray dots in Fig. 4, respectively, and calculate the corresponding average intensity of electric fields in Fig. 5(a). It is seen that the blue cross scatters, the red open circular scatters, and the black solid line almost overlap each other, which reveals the nearly position-independent mode splitting. In Figs. 5(b) and 5(c) we also show the effect of the loss in the ENZ medium on the mode splitting. With the increase of the loss, the split modes will be gradually weakened. However, even when the value of loss reaches 0.5, the spatially independent property of mode splitting still exists. Finally, we discuss the possibility of extending the 2D structure to a 3D case. When the 2D PhC cavity becomes a slab PhC cavity, e.g., the rod has a finite height of 1300 nm along z direction [20], we need to study whether the electric fields can be confined in the ENZ medium along z direction. Based on the Fresnel formula, the module of reflection coefficient at the interface from an ENZ medium to the air should be 1, owing to the sharp impedance mismatch between the two media. We further put an electric dipole source with working frequency of 175.4 THz at the center of a cube filled with ENG medium and simulate the electric fields using CST software. The center of the cube is assumed to be the origin of Cartesian coordinate system and each side of the cube is 1300 nm. In Figs. 6(a) and 6(b) we show the electric field patterns in x-z plane at y = 630 nm and in y-z plane at x = 630 nm, respectively. The region inside the solid lines denotes an ENG medium with $\varepsilon = 0.0001$, $\mu = 1$, and that outside the ENG medium is air. From Fig. 6, it is seen that the electric fields are trapped in the ENZ medium. The electric field patterns at other x-z and y-z planes all demonstrate the confinement of electric fields in the ENZ medium.

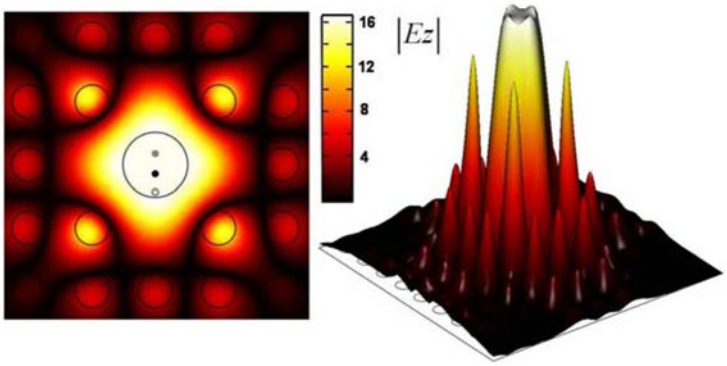

Fig. 4. 2D and 3D electric field patterns at a cavity mode of 175.4 THz. The circular zone denotes an ENZ medium. The white, the black and the gray dots indicate an oscillator located at three different places.

3. Experimental verifications in microwave regime

In practice, in nanometer scale regime our structure might be realized in a square-lattice-of-rod PhC slab with a defect rod of heavily doped semiconductor that can incorporate QDs. Owing to the limitations of our fabrication condition, we can only manufacture a system of two coupled

#159017 - $15.00 USD Received 1 Dec 2011; revised 25 Jan 2012; accepted 1 Mar 2012; published 5 Mar 2012

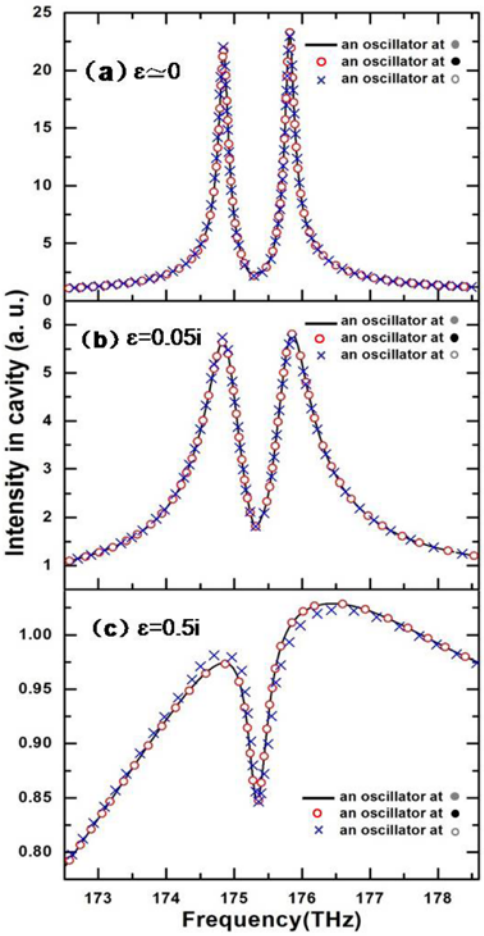

Fig. 5. Normal-mode splitting when an oscillator is put at three different places as indicated by the white, the black and the gray dots in the ENZ medium with varying degrees of loss, respectively.

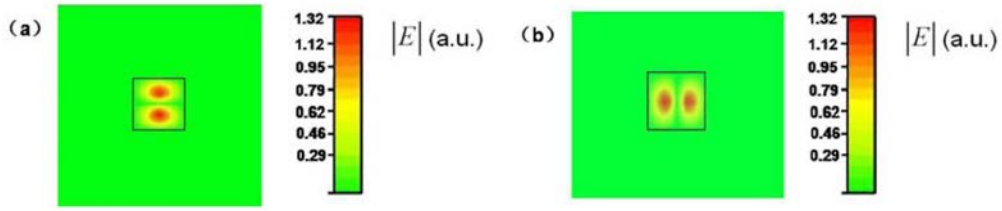

Fig. 6. Electric field patterns in x-z plane at y = 630 nm (a) and in y-z plane at x = 630 nm (b), respectively. The electric dipole source at frequency of 175.4 THz is put at the center of a cube filled with ENZ medium. Each side of the cube is 1300 nm.

oscillators in microwave regime, in which the semiconductor-based optical ZIM is changed to the transmission-line- based effective ZIM and the oscillator 1 in the nanometer scale size of a QD is changed to a magnetic resonator in the millimeter scale size. In the experiments, we utilize a composite right/left-handed transmission line with deep subwavelength unit cell to mimic a ZIM [18] and use a metallic split ring resonator (SRR) as a magnetic resonator whose

#159017 - $15.00 USD Received 1 Dec 2011; revised 25 Jan 2012; accepted 1 Mar 2012; published 5 Mar 2012

resonance frequency is determined by structural parameters and can be tuned by integrating additional lumped elements [26]. A SRR or other magnetic resonator, if coupled to inhomogeneous cavity fields, can result in position-dependent mode splitting [27,28]. Here a SRR was fabricated on a FR-4 substrate with a permittivity of 4.75 and a loss tangent of 0.012. The parameters of the SRR, as shown in the inset of Fig. 7(a), are a = t = 0.4 mm, w = 5 mm, b = 0.3 mm, c = 0.27 mm, d = 3 mm, L = 14 mm and h = 0.8 mm. In the slit of the outer ring, we load a ceramic trimmer capacitor to tune the resonance frequency. In Fig. 7, all the parameters of the ZIM-filled cavity are the same with those in reference [18] except that we use four unit cells to form the effective ZIM. The capacitance of the capacitor in the SRR is selected to be 0.77 pF to make the resonance frequency of SRR coincide with that of the cavity (1.12 GHz). Then the SRR is successively coupled to the ZIM at four different places, which are shown in Figs. 7(a)-7(d). Using Agilent Technologies' Advance-Design-System software, in Fig. 8(a) we calculate the transmission coefficient of four samples. The internal resistance in the capacitor in SRR is supposed to be $2\,\Omega$. It is seen that the previous cavity mode of 1.12 GHz splits into two modes after the SRR is coupled to the cavity. Moreover, the two split modes are nearly invariant when the SRR is put at four different places of the ZIM. In Fig. 8(b) we also show the measured transmission coefficient of four samples using Agilent 8722ES Vector Network Analysis. The measured results that in general agree well with the simulations demonstrate a nearly position-independent mode splitting.

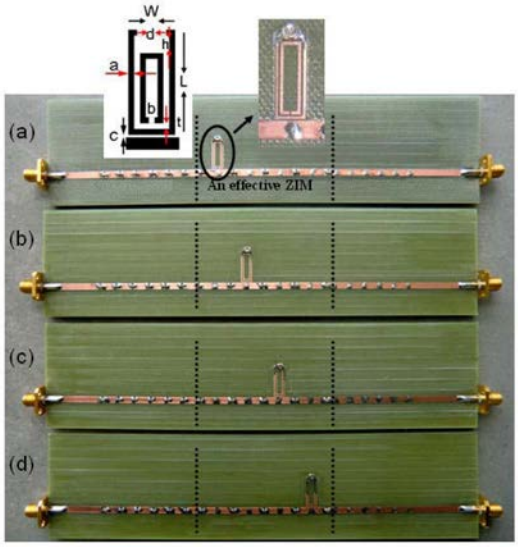

Fig. 7. Photograph of an effective ZIM coupled by a SRR at four different places, respectively. Inset of (a) is the layout of the SRR whose parameters are a = t = 0.4 mm, w = 5 mm, b = 0.3 mm, c = 0.27mm, d = 3 mm, L = 14 mm and h = 0.8 mm. The capacitance of the capacitor in the SRR is 0.77 pF.

#159017 - $15.00 USD Received 1 Dec 2011; revised 25 Jan 2012; accepted 1 Mar 2012; published 5 Mar 2012

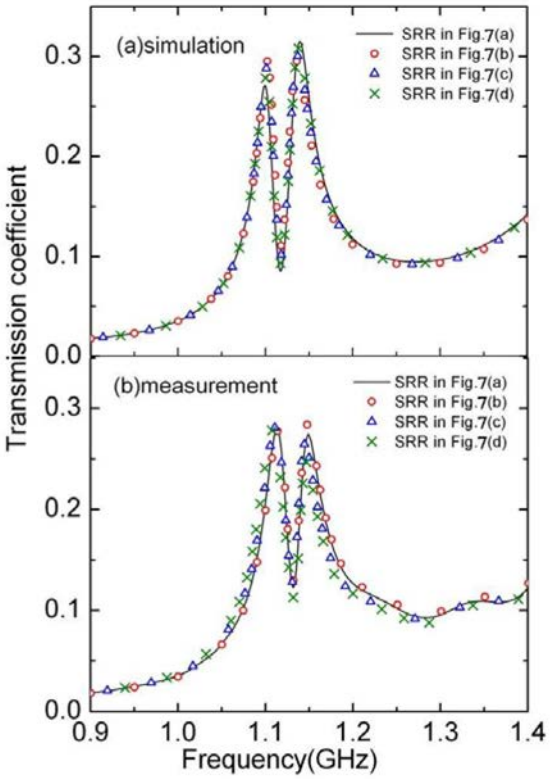

Fig. 8. Nearly position-independent mode splitting when a SRR is coupled to an effective ZIM at various locations.

4. Conclusions

In conclusion, the coupling of an oscillator and a ZIM-filled cavity was studied. Owing to the (almost) uniform cavity fields, (nearly) position-independent normal-mode splitting has been achieved. In the quantum limit for strongly coupled QD-cavity systems, the ZIM-filled cavity can avoid the positional uncertainty of QDs. A ZIM-filled cavity in the strong coupling regime will provide us a new platform to study the interactions of atoms and photons in the future.

Acknowledgments

The authors thank Y. W. Zhang, H. Q. Li, L He, and L. W. Zhang for their help in the experiments. This work was funded by the National Basic Research Program of China (grant 2011CB922001), from the National Natural Science Foundation of China (grant 11074187), and from the Program of the Shanghai Science and Technology Committee (grants 08dj1400301, 10ZR1431800 and 11QA1406900). Yasha Yi thanks the financial support from Army Research Office, National Science Foundation and MIT Microsystem Technology Laboratory.

#159017 - $15.00 USD Received 1 Dec 2011; revised 25 Jan 2012; accepted 1 Mar 2012; published 5 Mar 2012